World Academy of Science, Engineering and Technology
International Journal of Electrical and Computer Engineering
Vol:10, No:7, 2016

Performences of Type-2 Fuzzy Logic Control and Neuro-Fuzzy Control Based on DPC for Grid Connected DFIG with Fixed Switching Frequency

Fayssal Amrane, Azeddine Chaiba

***Abstract*—**In this paper, type-2 fuzzy logic control (T2FLC) and neuro-fuzzy control (NFC) for a doubly fed induction generator (DFIG) based on direct power control (DPC) with a fixed switching frequency is proposed for wind generation application. First, a mathematical model of the doubly-fed induction generator implemented in d-q reference frame is achieved. Then, a DPC algorithm approach for controlling active and reactive power of DFIG via fixed switching frequency is incorporated using PID. The performance of T2FLC and NFC, which is based on the DPC algorithm, are investigated and compared to those obtained from the PID controller. Finally, simulation results demonstrate that the NFC is more robust, superior dynamic performance for wind power generation system applications.

***Keywords*—**Doubly fed induction generetor, direct power control, space vector modulation, type-2 fuzzy logic control, neuro-fuzzy control, maximum power point tracking.

I. Introduction

MANY of the wind turbines installed today are equipped with DFIG. However, most of these machines are connected directly to the network to avoid the presence of a converter. The major advantage of these facilities lies in the fact that the power rate of the inverters is around the 25 % - 30 % of the nominal generator power [1], [2].

Essentially, the DFIG is a wound rotor induction generator (WRIG) whose stator windings are connected to the grid directly and rotor windings connected to the grid through back-to-back converter. A schematic diagram of variable speed wind turbine system with a DFIG is shown in Fig. 1. Control strategies of DFIG have been discussed in literatures [3], [4]. Control of DFIG through the Field Oriented Control (FOC) which is performed by rotor currents control has been developed in [5]. FOC method depends on parameters variation and its power dynamics can be influenced by these variations. Although, DFIG control using Input-Output Feedback Linearization method can operate below and above synchronous speed, but complication of control method and dependence on parameters are its disadvantages.

DPC strategy, as an alternative, has been introduced to the DFIG based wind power generation, the basic theory of DPC has been described in detail in [6], same as the well-known direct torque control strategy, the basic DPC has the demerits of large torque and current ripple and variable switching frequency, a space vector modulation based constant switching frequency DPC method is proposed in [7] to solve the previous problems, and some compensation method is proposed as well to improve the system performance. Further, three improved DPC methods, with different control targets, for DFIG control system have been discussed and implemented in [8]. During the past decade, various adaptive and robust controllers, based on variable structure controller [9], and fuzzy-neural techniques [10], [11] are proposed for electrical drives. Neuro-fuzzy systems combine the advantageous of neural networks and fuzzy logic systems.

In [12], the author has presented a model reference adaptive system (MRAS) speed estimator for speed sensorless direct torque and flux control (DTFC) of an induction motor drive (IMD), has proposed tow topologies based in Type-1 fuzzy logic controller (T1FLC) and T2FLC to achieve high performance sensorless drive in both transient as steady state conditions. In [13] a statistic study has proposed, which based on applications of fuzzy logic in renewable energy systems between 1994 until 2014, it is clear that the wind energy have big importance in these researches using neuro fuzzy, fuzzy particle swarm optimization, fuzzy genetic algorithms in simulation and experimental.

In this paper, T2FLC and NFC are used for adjusting rotor current of DFIG. This paper is organized as follows; firstly, the modeling of the turbine is presented in Section II. In Section III, the mathematical model of DFIG is given. Section IV presents DPC of DFIG which is based on the orientation of the stator flux vector along the axis ‘d’. The NFC and T2FLC are established to control the rotor currents are represented in Section V and Section VI, respectively. In Section VII, computer simulation results are shown and discussed. Finally, the reported work is concluded.

II. Model of the Turbine

The wind turbine input power usually is:

$$P_v = \frac{1}{2} * \rho * S_w * v^3 \quad (1)$$

where ρ is air density; S_w is wind turbine blades swept area in the wind; v is wind speed.

The output mechanical power of wind turbine is:

$$P_m = C_p * P_v = \frac{1}{2} * C_p * \rho * S_w * v^3 \quad (2)$$

Fayssal Amrane, Azeddine Chaiba are with the LAS Research Laboratory, Department of Electrical Engineering, University Ferhat Abbas Setif 1, Setif, Algeria (e-mail: amrane_fayssal@live.fr; chaiba_azeddine@yahoo.fr).

where *Cp* represents the wind turbine power conversion efficiency. It is a function of the tip speed ratio λ and the blade pitch angle β in a pitch-controlled wind turbine. λ is defined as the ratio of the tip speed of the turbine blades to wind speed. λ is given by:

$$\lambda = \frac{R*\Omega_t}{v} \quad (3)$$

where R is blade radius, Ωt is angular speed of the turbine. *Cp* can be described as [10], [11]:

$$C_p = \left(0.5 - 0.0167 * (\beta - 2)\right) * \sin\left[\frac{\pi*(\lambda+0.1)}{18.5-0.3*(\beta-2)}\right] - 0.00184 * (\lambda - 3) * (\beta - 2) \quad (4)$$

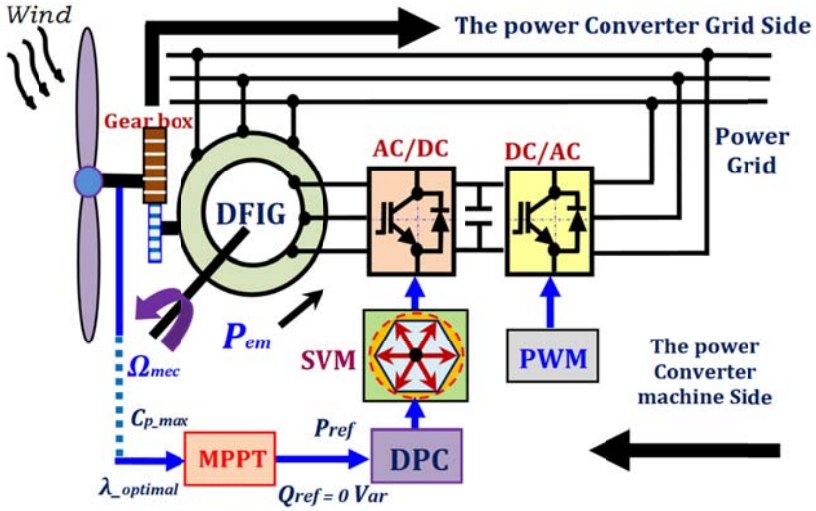

Fig. 1 Schematic diagram of wind turbine system with a DFIG

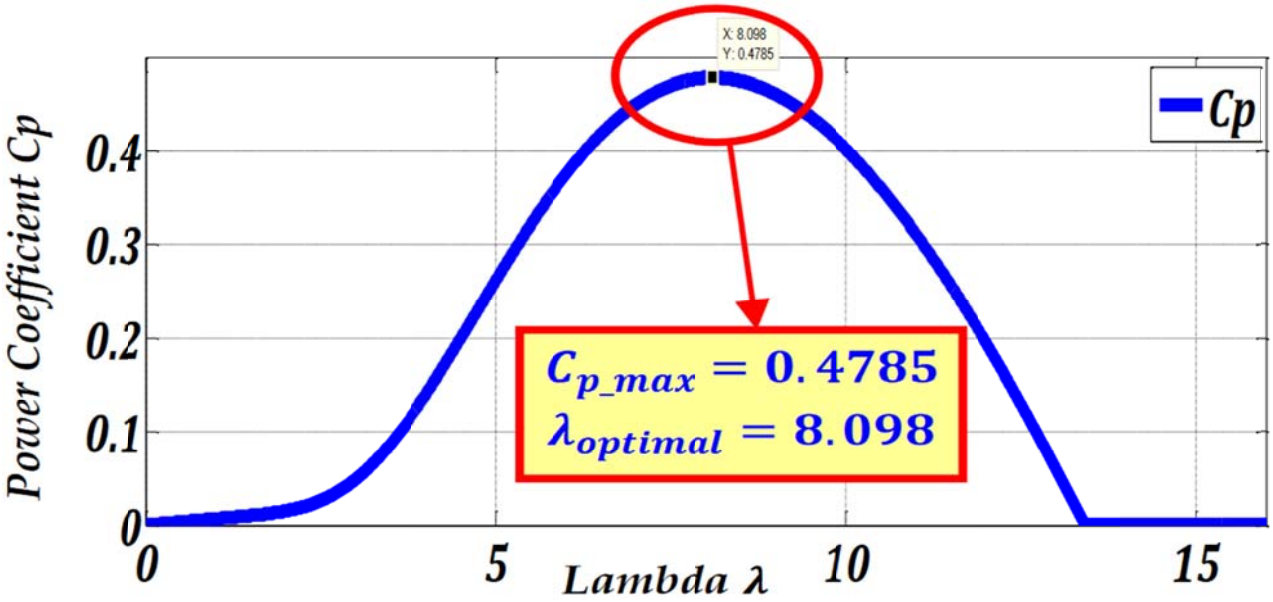

Fig. 2 Aerodynamic power coefficient variation Cp

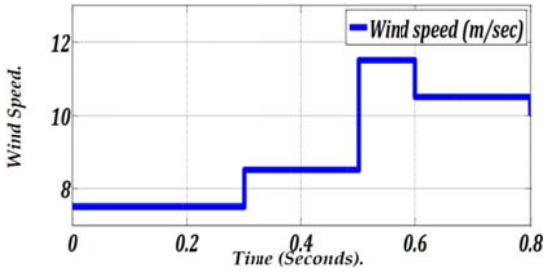

Fig. 3 Wind profile (Wind Speed)

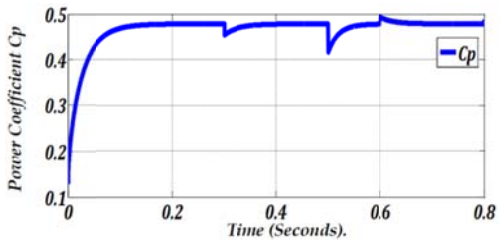

Fig. 4 Power coefficient (Cp)

The maximum value of Cp ($C_{p\_max} = 0.4785$) is achieved for $\beta = 0$ degree and for $\lambda_{opt} = 8.107$. This point corresponds at the maximum power point tracking (MPPT) [16].

In our work, we use the wind profile, as shown in Fig. 3.

After the simulation of the wind turbine using this wind profile, we test the robustness of our MPPT algorithm. As results the curve of power coefficient Cp versus time is shown in Fig. 4; this latter achieved the maximum value mentioned in Fig. 2 ($C_{p\_max} = 0.4785$) despite the variation of the wind.

III. Mathematical Model of DFIG

The generator chosen for the conversion of wind energy is a double-fed induction generator, DFIG modeling described in the two-phase reference by the following equations, [14], [15]:

Stator and rotor voltages:

$$V_{sd} = R_s * i_{sd} + \frac{d}{dt}\emptyset_{sd} - \omega_s * \emptyset_{sq} \quad (5)$$

$$V_{sq} = R_s * i_{sq} + \frac{d}{dt}\emptyset_{sq} + \omega_s * \emptyset_{sd} \quad (6)$$

$$V_{rd} = R_r * i_{rd} + \frac{d}{dt}\emptyset_{rd} - (\omega_s - \omega) * \emptyset_{rq} \quad (7)$$

$$V_{rq} = R_r * i_{rq} + \frac{d}{dt}\emptyset_{rq} + (\omega_s - \omega) * \emptyset_{rd} \quad (8)$$

Stator and rotor fluxes:

$$\emptyset_{sd} = L_s * i_{sd} + L_m * i_{rd} \quad (9)$$

$$\emptyset_{sq} = L_s * i_{sq} + L_m * i_{rd} \quad (10)$$

$$\emptyset_{rd} = L_r * i_{rd} + L_m * i_{sd} \quad (11)$$

$$\emptyset_{rq} = L_r * i_{rd} + L_m * i_{sd} \quad (12)$$

The electromagnetic torque is given by:

$$C_e = P * L_m * (i_{rd} * i_{sq} - i_{rq} * i_{sd} \quad (13)$$

and its associated motion equation is:

$$C_e - C_r = J * \frac{d}{dt}\Omega + f * \Omega \quad (14)$$

$$J = \frac{J_{turbine}}{G^2} + J_g \quad (15)$$

where C_r is the load torque J is total inertia in DFIG's rotor, Ω is mechanical speed and G is gain of gear box.

The voltage vectors, produced by a three-phase PWM inverter, divide the space vector plane into six sectors, as shown in Fig. 5 [17].

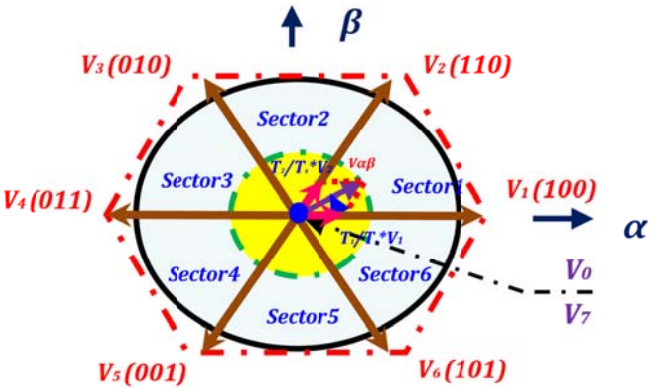

Fig. 5 The diagram of voltage space vectors in *α-β* plan

In every sector, each voltage vector is synthesized by the basic space voltage vector of the two sides of the sector and one zero vector. For example, in the first sector, V$\boldsymbol{\alpha\beta}$ is a synthesized voltage space vector and is expressed by:

$$\vec{V}_{\alpha\beta} = \frac{T_1}{T_S} * \vec{V_1} + \frac{T_2}{T_S} * \vec{V_2} \quad (16)$$

IV. DPC of DFIG

In this section, the DFIG model can be described by the following state equations in the synchronous reference frame whose axis *d* is aligned with the stator flux vector as shown in Fig. 6, ($\emptyset_{sd} = \emptyset_s$)and ($\emptyset_{sq} = 0$) [6].

By neglecting resistances of the stator phases the stator voltage will be expressed by:

$$V_{sd} = 0 \; and \; V_{sq} = V_s \cong \omega_s * \emptyset_s \quad (17)$$

We lead to an uncoupled power control; where, the transversal component *irq* of the rotor current controls the active power. The reactive power is imposed by the direct component *ird* as in shown in Fig. 7:

$$P_s = -V_s * \frac{L_m}{L_s} * i_{rq} \quad (18)$$

$$Q_s = \frac{V^2{}_s}{\omega_s * L_s} - V_s * \frac{L_m}{L_s} * i_{rd} \quad (19)$$

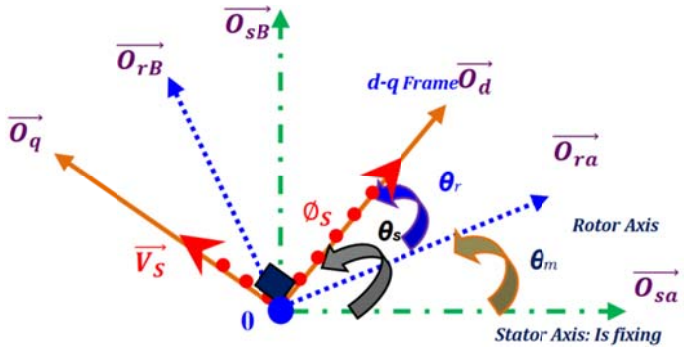

Fig. 6 Stator and rotor flux vectors in the synchronous d-q frame.

The arrangement of the equations gives the expressions of the voltages according to the rotor currents:

$$V_{rd} = R_r * i_{rd} + \left(L_r - \frac{L_m^2}{L_s}\right) * \frac{di_{rd}}{dt} - g * \omega_s * \left(L_r - \frac{L_m^2}{L_s}\right) * i_{rq} \quad (20)$$

$$V_{rq} = R_r * i_{rq} + \left(L_r - \frac{L_m^2}{L_s}\right) * \frac{di_{rq}}{dt} + g * \omega_s * \left(L_r - \frac{L_m^2}{L_s}\right) * i_{rd} + g * \frac{L_m * V_s}{L_s} \quad (21)$$

$$i_{rd} = -\frac{1}{\sigma * \tau_r} * i_{rd} + g * \omega_s * i_{rq} + \frac{1}{\sigma * L_r} * V_{rd} \quad (22)$$

$$i_{rq} = -\frac{1}{\sigma}\left(\frac{1}{\tau_r} + \frac{L_m^2}{L_s * T_s * L_r}\right) * i_{rq} - g * \omega_s * i_{rd} + \frac{1}{\sigma * L_r} * V_{rq} \quad (23)$$

with:

$$T_r = \frac{L_r}{R_r};\ T_s = \frac{L_s}{R_r};\ \sigma = 1 - \frac{L_m^2}{L_s * L_r} \quad (24)$$

where; ϕ_{sd}, ϕ_{sq} are stator flux components, ϕ_{rd}, ϕ_{rq} are rotor flux components, V_{sd}, V_{sq} are stator voltage components, V_{rd}, V_{rq} are rotor voltage components. R_s, R_r are stator and rotor resistances, L_s, L_r are stator and rotor inductances, L_m is mutual inductance, σ is leakage factor, P is number of pole pairs, $\omega_s$is the stator pulsation, ω is the rotor pulsation, f is the friction coefficient, T_s and T_r are stator and rotor time-constant, and g is the slip.

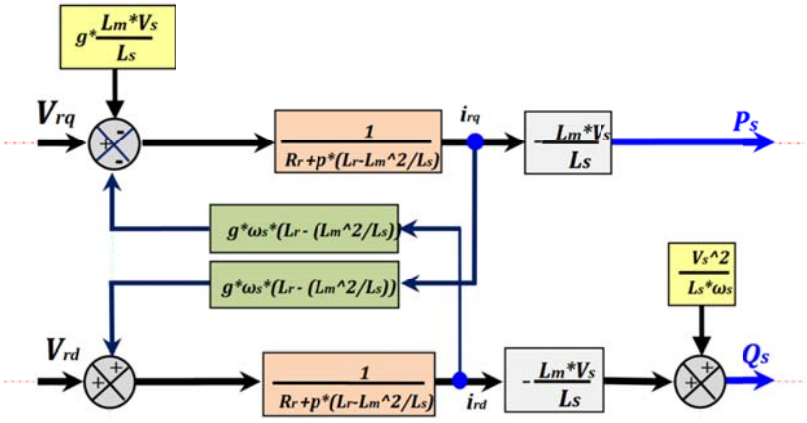

Fig. 7 DFIG simplified model

V. Design of NFC Controller

The block diagram of the NFC system is shown in Fig. 8. The NFC controller is composed of an on-line learning algorithm with a neuro-fuzzy network. The neuro-fuzzy network is trained using an on-line learning algorithm. The NFC has two inputs, the rotor current error e_{idr} and the derivative of rotor current error $\dot{e}_{idr}$. The output is rotor voltage V_{dr}. For the NFC of rotor current i_{rq} is similar with i_{rd} controller [10].

A. Description of NFC

For the NFC, a four layer NN as shown in Fig. 9 is used. Layers I–IV represents the inputs of the network, the membership functions, the fuzzy rule base and the outputs of the network, respectively [10].

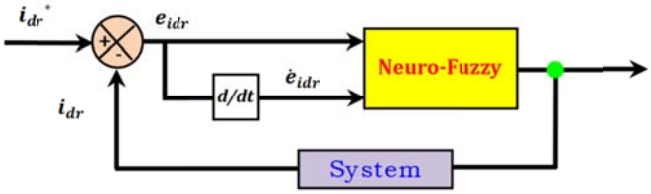

Fig. 8 Block diagram of NFC

The proposed DPC of a DFIG based on NFC is shown in Fig. 10.

VI. Design of T2FLC

T2FLC used in this work has two inputs and one output. The membership functions are defined in Figs. 11 (a) and (b). The fuzzy rule base consists of a collection of linguistic rules of the form [12], [13].

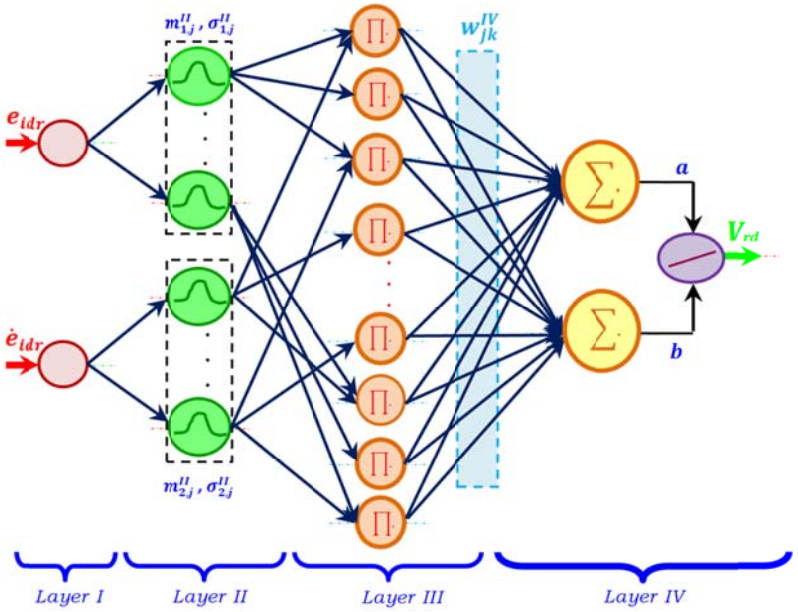

Fig. 9 Schematic diagram of the neuro-fuzzy network

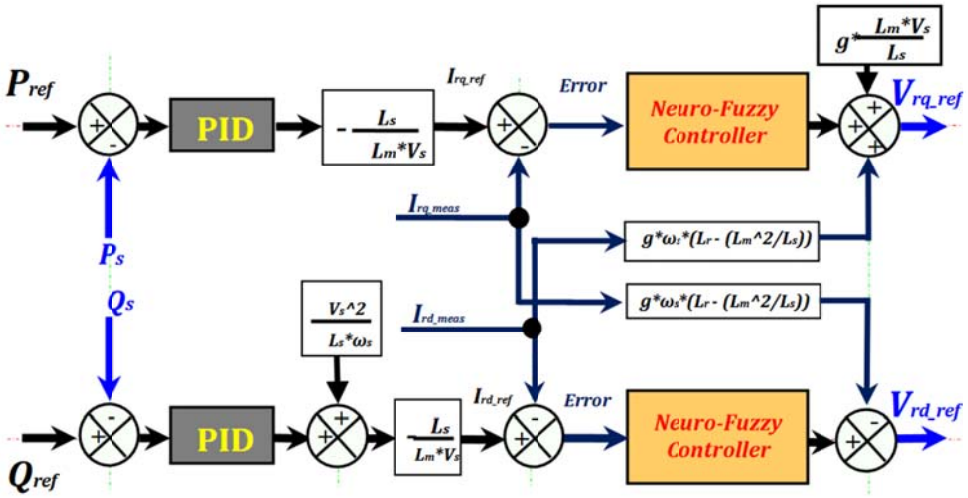

Fig. 10 Proposed DPC using NFC

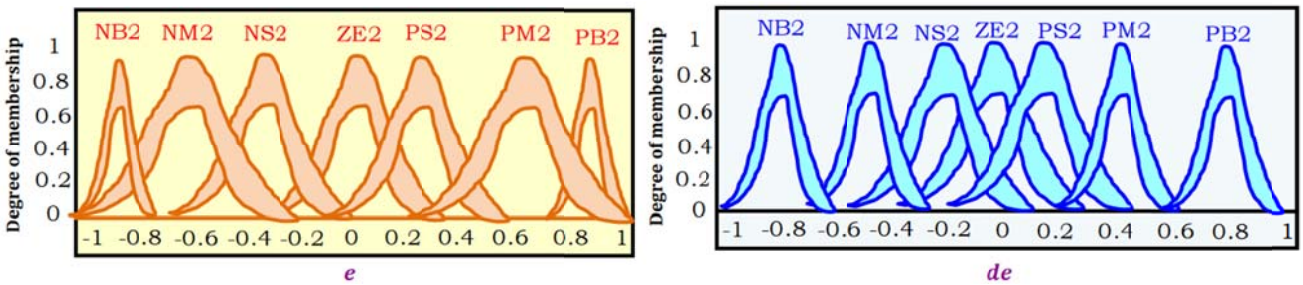

(a) Inputs membership functions

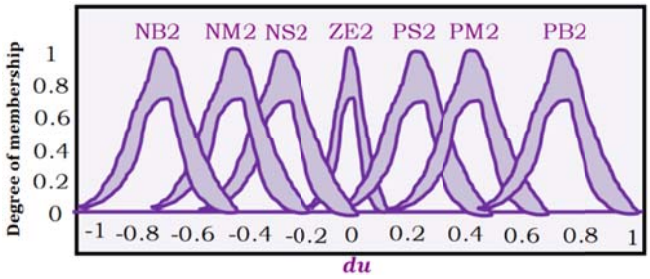

(b) Output membership functions

Fig. 11 Membership functions

Rule 1: if $S_{1,2}$ is NB2, and $S_{1,2}$ is NB2 then $dU_{1,2}$ is NB2.
Rule 2: if $S_{1,2}$ is NM2, and $S_{1,2}$ is NB2 then $dU_{1,2}$ is NB2.
Rule 3: if $S_{1,2}$ is NS2, and $S_{1,2}$ is NG2 then $dU_{1,2}$ is NS2.
⋮
Rule 49: if $S_{1,2}$ is PB2, and $S_{1,2}$ is PB2 then $dU_{1,2}$ is PB2.

These inferences can be made in a more explain as shown in Table I [12],[13].

TABLE I
TYPE-2 FUZZY INFERENCE TABLE

$dU_{1,2}$	$dS_{1,2}$						
	NB2	**NM2**	**NS2**	**EZ2**	**PS2**	**PM2**	**PB2**
NB2	NB2	NB2	NB2	NM2	NS2	NS2	**EZ2**
NM2	NB2	NM2	NM2	NM2	NS2	**EZ2**	PS2
NS2	NB2	NM2	NS2	NS2	**EZ2**	PS2	PM2
EZ2	NB2	NM2	NS2	**EZ2**	PS2	PM2	PM2
PS2	NM2	NS2	**EZ2**	PS2	PS2	PM2	PB2
PM2	NS2	**EZ2**	PS2	PM2	PM2	PM2	PB2
PB2	**EZ2**	PS2	PS2	PM2	PB2	PB2	PB2

dS1,2

The equivalent scheme of t T2FLC for adjusting rotor currents of DPC in this work is shown in Fig. 12. The proposed DPC of a DFIG based on T2FLC is shown in Fig. 13. The overall system is described in detail, as shown in Fig. 14.

VII. SIMULATION RESULTS

The DFIG used in this work is a *4 kW* whose nominal parameters are indicated in Table III. And the wind turbine is a *10 kW* whose parameters are indicated in Table IV.

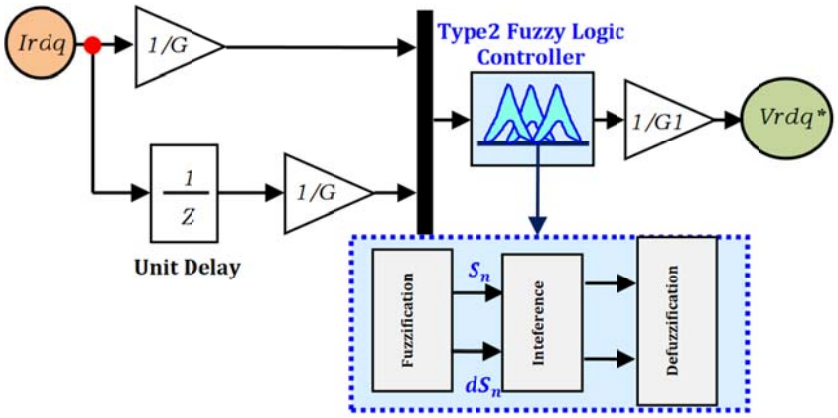

Fig. 12 The Simulink scheme of T2FLC for rotor currents

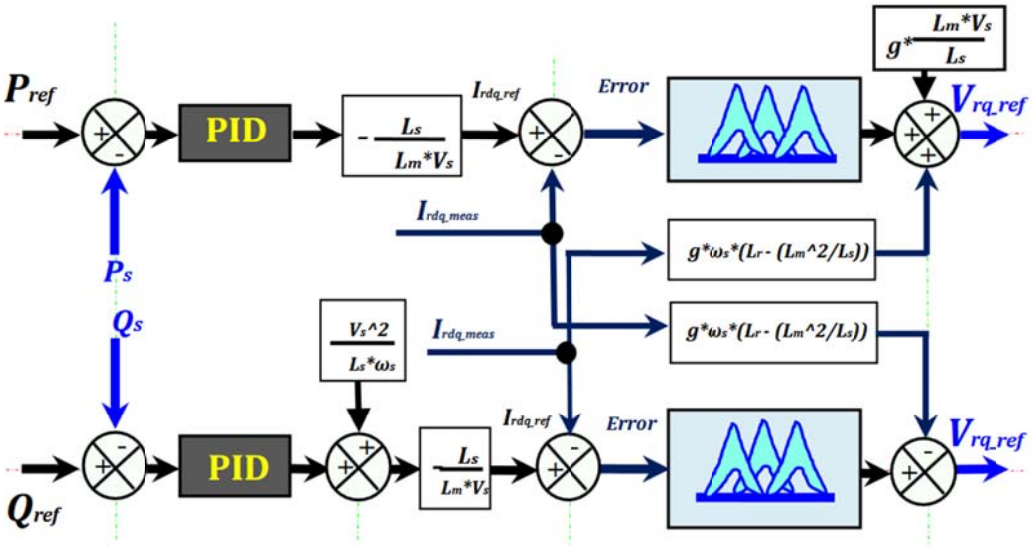

Fig. 13 The proposed DPC using T2FLC

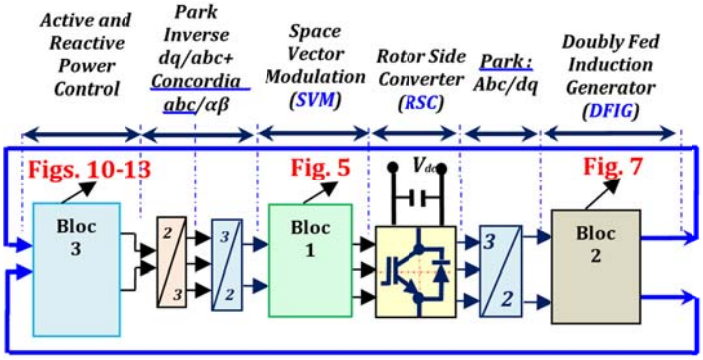

Fig. 14 Global system

For both cases, we use robustness test as follows:

- Case I (NFC)

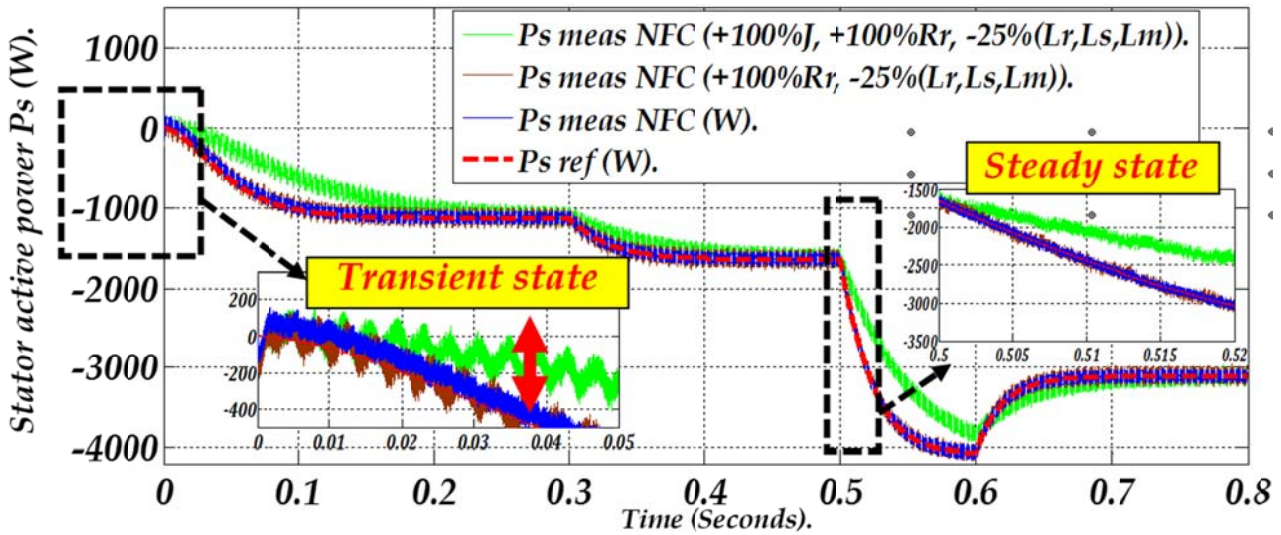

Fig. 15 Stator active power Ps.

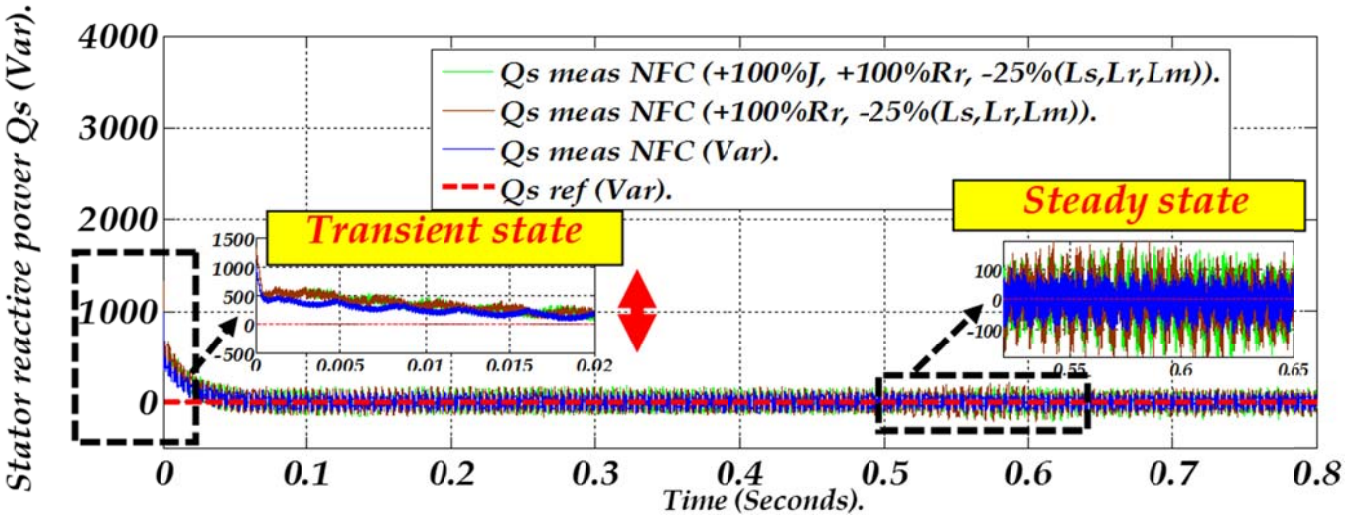

Fig. 16 Stator reactive power QS

- Case II (T2FLC)

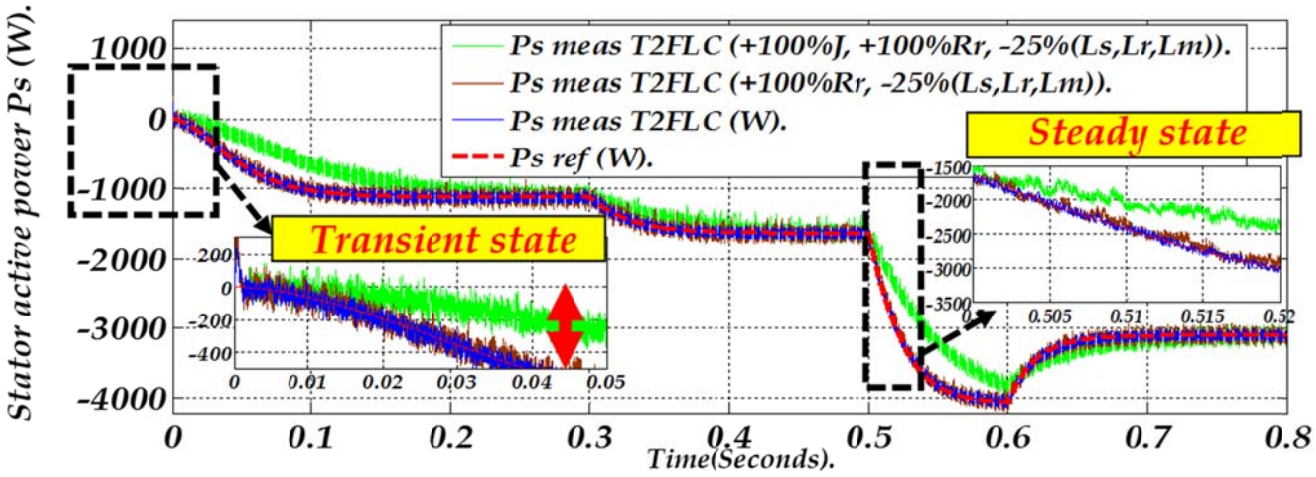

Fig. 17 Stator active power Ps

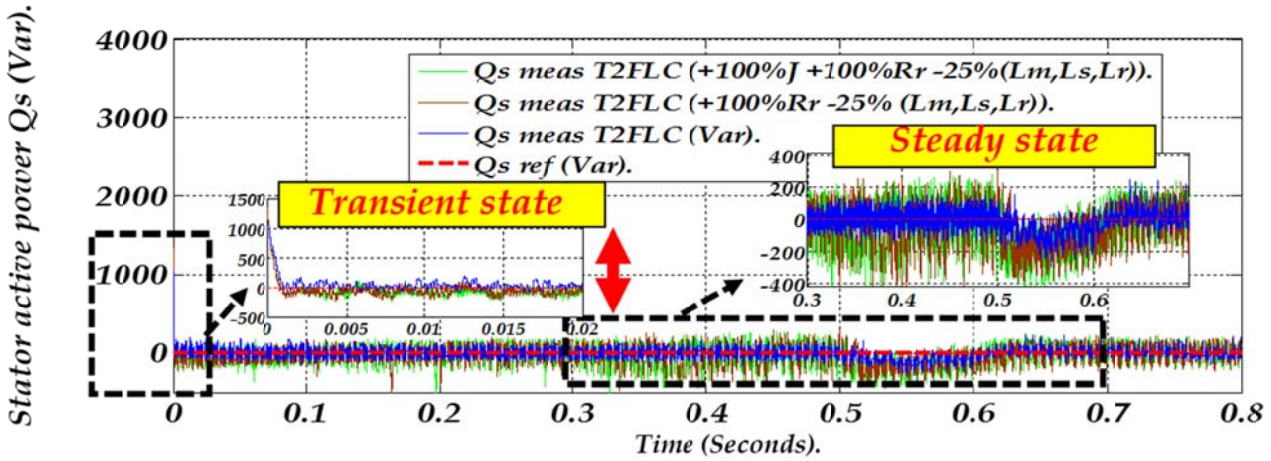

Fig. 18 Stator reactive power QS

Test 1: (Without robustness test) → *Blue color*.
Test 2: Add ***100%*** *for Rr,* and decrease ***25%*** for *Ls, Lr,* and *Lm* → *Brown color*.
Test 3: Add ***100 %*** *for Rr* and *J,* and decrease ***25%*** for *Ls, Lr,* and *Lm* → *Green color*

Figs. 15 and 17 represent the stator active power injected into the grid using SVM for proposed control using NFC and T2FLC, respectively, via MPPT strategy. It can be said that the stator active power follows exactly its reference, for both proposed controls (Test1-blue color). After a robustness test (Test 2-brown color), the stator active power follows its reference, but we note that there are few ripples in the proposed T2FLC and neglected in NFC. After adding +100 % of the moment inertia J, a remarkable power error is noted, with severe disruptions; only in the proposed control using T2FLC (Test3-green color) between 0.5 sec until 0.52 sec.

TABLE II
RESULTS'S RECAPITULATION

	NFC	*T2FLC*
Stator Current's THD	***0.78 %***	***1.14 %***
Rotor Current's THD	***2.80 %***	***13.77 %***
Power's error	***+/- 110 (W_VAR)***	***+/- 130(W_VAR)***

TABLE III
PARAMETERS OF THE DFIG

Rated Power:	*4 Kwatts*
Stator Resistance:	*Rs = 1.2Ω*
Rotor Resistance:	*Rr = 1.8Ω*
Stator Inductance:	*Ls = 0.1554 H.*
Rotor Inductance:	*Lr = 0.1558 H.*
Mutual Inductance:	*Lm = 0.15 H.*
Rated Voltage:	*Vs = 220/380 V*
Number of Pole pairs:	*P= 2*
Rated Speed:	*N=1440 rpm*
Friction Coefficient:	*fDFIG=0.00 N*m/sec*
The moment of inertia	*J=0.2 kg*m^2*
Slid:	*g=-0.04*

TABLE IV
PARAMETERS OF THE TURBINE

Rated Power:	*10 Kwatts*
Number of Pole pairs:	*P= 3*
Blade diameter	*R= 3m*
Gain:	*G=5.4*
The moment of inertia	*Jt=0.00065 kg*m^2*
Friction coefficient	*ft=0.017 N*m/sec*
Air density:	*ρ=1.22 Kg/m^3*

VIII. CONCLUSION

In this paper neuro-fuzzy logic control and T2FLC for DFIG based on DPC with a fixed switching frequency have been proposed for wind generation application. DPC via SVM strategy has been achieved by adjusting active and reactive powers and rotor currents. The performances of NFC and T2FLC which is based on the DPC algorithm has been investigated and compared to those obtained from the PID controller for power control. The results obtained by the validation platform using the $MATLAB\ /\ Simulink^{®}$, have shown that the *NFC* has high efficiency, low error, very short response time, high dynamics for wind generation.

REFERENCES

[1] R. Pena, et al., "Doubly Fed Induction Generator using Back-to-Back PWM Converter and Its Application to Variable-Speed Wind–Energy Generation", IEE Proc. B, vol. 143, no.3, pp.231-241,1996.
[2] S. Muller, M. Deicke, R.W. D. Doncker, "Doubly fed induction generator systems for wind turbines", IEEE Industry Application Magazine, Vol.8, No.3, pp. 26-33.2002.
[3] J. Ben Alaya, A. Khedher and M. F. Mimouni, " DTC, DPC and Nonlinear Vector Control Strategies Applied to the DFIG operated at Variable Speed", Journal of Electrical Engineering (.lEE), vol. 6, no II, pp. 744-753,2011.
[4] Luna, F. K. A Lima, P. Rodriguez, E. H. Watanabe and R.Teodorescu, "Comparison of Power Control Strategies for DFIG Wind Turbines", IEEE Trans on Energy Conversion, pp. 2131-2136, 2008.
[5] AG. Abo-Khalil, G. Ahmed, "Synchronization of DFIG output voltageto utility grid in wind power system", Renewable Energy 44, pp. 193-198,2012.
[6] L. Xu, P. Cartwright. "Direct Active and Reactive Power Control of DFIG for Wind Energy Generation", IEEE Trans. on energy conversion, vol.21,pp.750-758.
[7] D. W. Zhi, L. Xu. "Improved Direct Power Control of Doubly-Fed Induction Generator Based Wind Energy System", IEMDC2007,pp.436-441.
[8] M. Guo, D. Sun, B. T. He, "Direct Power Control for Wind-Turbine Driven DFIG with Constant Switch Frequency", ICEMS 2007,pp.1966-1971.
[9] Qingding, G. Limei. W & Ruifu, L. Robust fuzzy variable structure control of PMLSM servo system, IEEE International conference on intelligent processing systems, Beijing, China. 675-679. 1997.
[10] Elmas, C., Ustun, O. & Sayan, H. H, A neuro-fuzzy controller for speed control of a permanent magnet synchronous motor drive.. Expert Systems with Applications, 34.1, 657-664. 2008.
[11] Gökbulut, M., Dandil, B; & Bal, C., A hybrid neuro-fuzzy controller for brushless DC motors. Lecture Notes in Computer Science, 3949. 125-132. 2006
[12] Tejavathu Ramesh n, AnupKumarPanda, S.ShivaKumar, "Type-2 fuzzy logic control based MRAS speed estimator for speed sensorless direct torque and flux control of an induction motor drive", ISA Transactions 2015.
[13] L. Suganthi a,n, S.Iniyan b, AnandA.Samuel c, "Applications of fuzzy logic in renewable energy systems – A review", Renewable and Sustainable Energy Reviews 48, 2015, pp. 585–607.
[14] Gaillard A, Karimi S, Poure P, Saadate S. Fault tolerant back-to-back converter topology for wind turbine with doubly fed induction generator. International Review of Electrical Engineering Aug. 2007:629–36.
[15] Lie Xu Cartwright P. Direct active and reactive power control of DFIG for wind energy generation. IEEE Transactions on Energy Conversion Sept. 2006;21(3): 750–8.
[16] Hong YY, Lu SD, Chiou CS. MPPT for PM wind generator using gradient approximation. Energy Convers Manage 2009;50:82–9.
[17] Zhi D, Xu L. Direct power control of DFIG with constant switching frequency and improved transient performance. IEEE Trans Energy Convers2007;22(1):110–8.